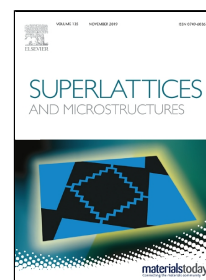


Spin transport in proximity-induced ferromagnetic phosphorene nanoribbons

Junsong Jiang, Qingtian Zhang, Zhongfei Mu, Kwok Sum Chan



PII: S0749-6036(19)31306-0  
DOI: <https://doi.org/10.1016/j.spmi.2019.106324>  
Reference: YSPMI 106324

To appear in: *Superlattices and Microstructures*

Received Date: 24 July 2019  
Accepted Date: 25 October 2019

Please cite this article as: Junsong Jiang, Qingtian Zhang, Zhongfei Mu, Kwok Sum Chan, Spin transport in proximity-induced ferromagnetic phosphorene nanoribbons, *Superlattices and Microstructures* (2019), <https://doi.org/10.1016/j.spmi.2019.106324>

This is a PDF file of an article that has undergone enhancements after acceptance, such as the addition of a cover page and metadata, and formatting for readability, but it is not yet the definitive version of record. This version will undergo additional copyediting, typesetting and review before it is published in its final form, but we are providing this version to give early visibility of the article. Please note that, during the production process, errors may be discovered which could affect the content, and all legal disclaimers that apply to the journal pertain.

# Spin transport in proximity-induced ferromagnetic phosphorene nanoribbons

Junsong Jiang,<sup>1</sup> Qingtian Zhang,<sup>1,a)</sup> Zhongfei Mu<sup>2</sup> and Kwok Sum Chan<sup>3, a)</sup>

<sup>1</sup> School of Materials and Energy, Guangdong University of Technology, Guangzhou, Guangdong 510006, People's Republic of China.

<sup>2</sup> Experimental Teaching Department, Guangdong University of Technology, Guangzhou 510006, People's Republic of China

<sup>3</sup> Department of Physics and Materials Science, City University of Hong Kong, Tat Chee Avenue, Kowloon, Hong Kong, People's Republic of China

## Abstract

We investigate the spin-dependent transport properties in normal/ferromagnetic/normal phosphorene nanoribbon (PNRs) junctions where an external gate electrode is attached to the ferromagnetic region. The exchange splitting in ferromagnetic phosphorene is induced by ferromagnetic proximity effect. We found that the current through this junction is spin polarized due to the exchange field induced in phosphorene. The spin polarization oscillates with the external gate voltage, and the spin polarization can be reversed from 100% to -100% by a slight change of the gate voltage. The controllable spin transport in phosphorene nanoribbons can have useful applications in the development of spintronic devices.

**Keywords:** phosphorene; spin-dependent transport; spin polarization; spintronics

a) Authors to whom correspondence should be addressed: Email addresses:

[qtzhang@mail.ustc.edu.cn](mailto:qtzhang@mail.ustc.edu.cn), [apkschan@cityu.edu.hk](mailto:apkschan@cityu.edu.hk)

## Introduction

Two-dimensional (2D) layered crystal materials such as graphene[1, 2], MoS<sub>2</sub>[3-5], silicene[6-9] and transition metal dichalcogenides (TMDs)[3, 10, 11] have attracted a tremendous interest in recent years owing to their probable applications in electronic and spintronic devices. Recently, phosphorene, a newly discovered 2D semiconducting material, has drawn considerable attention from the research community[12-15]. Phosphorene is a monolayer black phosphorus (BP) and it has been fabricated from the bulk BP by using mechanical exfoliation method[12, 13]. BP is a layered material, similar to graphite, in which the individual layers are stacked by van der Waals interactions. In a single BP layer, based on  $sp^3$  hybridization, each phosphorus atom is covalently bonded to three other neighbors to form a corrugated honeycomb structure[16]. As is well-known, graphene has no band gap, which limits its applications in nanoelectronics[17]. Nevertheless, experiments show that phosphorene has a direct band gap from 1.5 eV of monolayer phosphorene to 0.3 eV of multilayer phosphorene[16, 18]. A few layers of phosphorene has been regarded as a preferable material for electronic device applications because it has a much larger mobility than MoS<sub>2</sub>, up to 1000 cm<sup>2</sup>/Vs[12-14, 19], and an on/off ratio up to 10<sup>5</sup> at room temperature makes it as a promising candidate for the field-effect transistor (FET). At present, various studies have been investigated theoretically and experimentally on phosphorene such as electronic, thermal, mechanical, optical and transport properties[20-26].

Similar to other 2D materials, PNRs can be segmented into two typical crystal ribbons, namely armchair-PNRs (APNRs) and zigzag-PNRs (ZPNRs) in different directions. It has been found that pristine APNRs are semiconductors with an indirect band gap, while their ZPNRs counterparts are metals regardless of the ribbon

width[27]. Unlike graphene which possesses a perfect planar structure, phosphorene possesses a buckled structure with a vertical distance between the two sublattice planes. So the transport properties of PNRs can be controlled by applying an electric field perpendicular to PNRs.

Phosphorene has been regarded as a promising candidate for spintronic-based devices due to its long spin lifetimes[28]. Phosphorene is a non-magnetic material, but it can be changed to be a ferromagnetic material by the proximity of ferromagnetic layers, which has been reported in graphene[29, 30]. Chen et al found that a large exchange splitting can be induced in phosphorene by depositing a EuO ferromagnetic stripe, and the value of exchange splitting is estimated to be 0.184 eV [31]. Keshtan et al investigated the spin filtering effects of ZPNRs in the presence of exchange splitting induced by the proximity of ferromagnetic stripes[32]. Fu et al proposed a spin-Seebeck diode in adatoms decorated ZPNRs[33]. In this work, we study the spin-polarized transport in monolayer phosphorene nanoribbons in the presence of a ferromagnetic stripe and an external gate voltage. The ferromagnetic stripe can induce an exchange splitting in phosphorene, and it is also used as a top gate for the applied electric potential. It is found that a 100% spin polarization can be obtained in both ZPNRs and APNRs. Moreover, the spin polarization in APNRs oscillates periodically with respect to the gate voltage, and a slight change of the gate voltage can reverse the spin polarization from -100% to 100%.

## Model and Methods

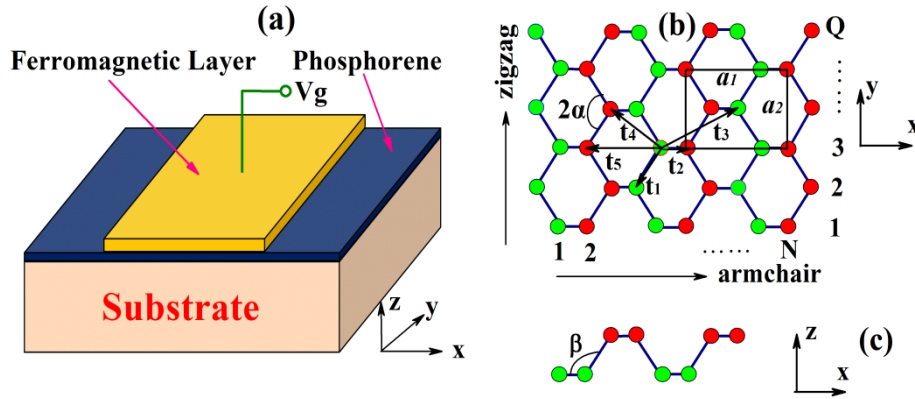


**Fig. 1.** (a) Schematic illustration of one ferromagnetic stripe is deposited on the monolayer phosphorene. (b) Top and (c) Side views of the lattice structure of monolayer phosphorene. The size of the device denoted by the ribbon length  $N$  and width  $Q$ .

The schematic illustration of our proposed device is shown in Fig. 1(a). A PNR is put on a substrate, and a ferromagnetic stripe is deposited on the PNR. The ferromagnetic stripe is also used as top gate for applying gate voltage. Top view of phosphorene lattice structure is shown in Fig. 1(b), and each unit cell consists four inequivalent phosphorus atoms. In tight-binding Hamiltonian, there are five transfer energies in phosphorene, which is indicated by  $t_i (i=1,2,\dots,5)$  in Fig. 1(b). The lengths of unit cell along the  $x$  and  $y$  directions can be shown by  $(a_1, a_2) = (0.443, 0.327)$  nm[14]. Side view of the lattice structure is presented in Fig. 1(c). The dimensions of the device can be described by the ribbon length  $N$  along the armchair edge and ribbon width  $Q$  along the zigzag edge. In our numerical study, the size for armchair phosphorene nanoribbon is chosen to be  $N = 32$ ,  $Q = 21$  ( $L_x=7.0$ nm  $L_y=3.3$  nm), and

the size for zigzag phosphorene nanoribbon is chosen to be  $N = 20$ ,  $Q = 33$  ( $L_x=4.4$  nm,  $L_y=5.2$  nm). Since our interest is in nano-scale devices, the device regions we studied have dimensions in the nano-meter range and require reasonable computation time.

In the tight-binding approximation, the Hamiltonian for PNRs with gate potential and exchange splitting can be given by

$$H = \sum_{i,\alpha} (\varepsilon_i + V_g) c_{i\alpha}^\dagger c_{i\alpha} + M \sum_{i,\alpha} c_{i\alpha}^\dagger \sigma_z c_{i\alpha} + \sum_{i,j,\alpha} t_{ij} c_{i\alpha}^\dagger c_{j\alpha} \quad (1)$$

where the summation runs over the lattice sites of PNRs.  $\varepsilon_i$  is the onsite energy of an electron at site  $i$ ,  $V_g$  is the gate potential,  $M$  is the exchange splitting induced by the ferromagnetic stripe,  $\sigma_z$  is the Pauli matrix, and  $c_{i\alpha}^\dagger (c_{j\alpha})$  is the creation (annihilation) operator of an electron with spin  $\alpha$  at site  $i(j)$ . The last term is the hopping links between phosphorus atoms, and the five hopping integrals are[34]:  $t_1 = -1.220$  eV,  $t_2 = 3.665$  eV,  $t_3 = -0.205$  eV,  $t_4 = -0.105$  eV,  $t_5 = -0.055$  eV. The tight-binding model we used was developed in[34] by fitting the model to the band structures calculated using the first principle method with GW approximation and the experimental lattice structure. The trend of the band gaps in the first principle band structures obtained for one layer to four layer phosphorene agree with the experimental observation, which supports the reliability of the model. As a result, the model has been used in a number of studies of the physical properties of phosphorene [32, 35-38]. Regarding the exchange parameter used in the model, despite the interest in spintronics, there is no experimental result for the proximity effect in phosphorene

and we have to rely on first principle prediction for the value of the exchange splitting. The value we used was obtained using first principle in Ref[31]. The tight-binding model for our proposed system is constructed by a python package Kwant[39], and Kwant libraries are called in the programs to calculate the band structure, density of states (DOS), and the conductance of the system under consideration. After we obtain the spin resolved conductance using Kwant, the spin polarization can be calculated by

$$P_s = \frac{G_{\uparrow} - G_{\downarrow}}{G_T} \quad (2)$$

where  $G_{\uparrow} (G_{\downarrow})$  is conductance for spin up(down) electron, and  $G_T$  is the total conductance, which is defined as  $G_T = G_{\uparrow} + G_{\downarrow}$ .

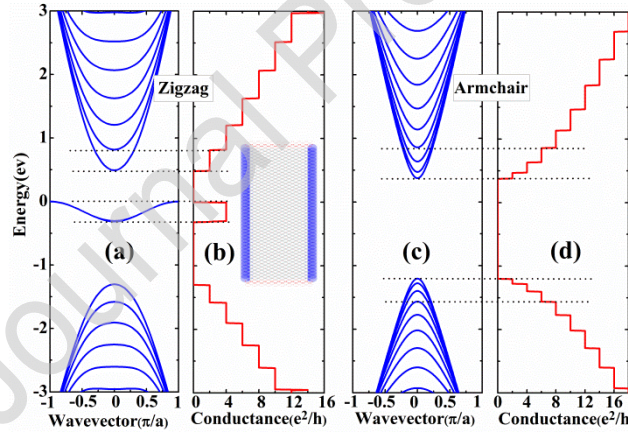


**Fig. 2.** The band structure and conductance for PNRs in the absence of an exchange field ( $M = 0$ ) and gate voltage ( $V_g = 0$ ). (a) and (b) The band structure and conductance for the ZPNRs. (c) and (d) The band structure and conductance for the APNRs. The inset in (b) is the local density of states (LDOS) for ZPNR at  $E_F = -0.2$  eV.

Firstly, we consider the band structures and conductances for ZPNRs (see Figs.

2(a) and (b)) and APNRs (see Figs. 2(c) and (d)). Here the exchange splitting and gate potential are set to be zero, and we only focus on the electronic properties of pristine PNRs. In Fig. 2(a), we can see a band in the energy region:  $-0.3 \text{ eV} < E_F < 0$ , and the band in the gap actually consists of two separate bands (ignoring the spin degeneracy), which are so close that their separation cannot be seen in the figure. When the spin degrees of freedom are considered, we will have four conduction channels in the energy region. It is noted that the conductance in this region is  $4e^2/h$ . The LDOS at Fermi energy  $E_F = -0.2 \text{ eV}$  for the ZPNRs is presented in the inset of Fig. 2(b). We can see that the LDOS only exists at the two edges of the ZPNRs, so electrons transport along the zigzag edges. In the zigzag ribbon band structure calculated, the pristine Fermi energy lies at the top of the band inside the gap (at zero energy). However, the Fermi energy can be moved inside the band in the gap, for example, by using a gate voltage to make the ribbon conductive. However, a band gap is found in the band structure of APNRs (see Fig.2(c)), which means that APNRs are semiconductors. We note that many subbands in both ZPNRs and APNRs, and each subband corresponds to a quantized one-dimensional conduction channel. Here the spin degrees of freedom are considered, so the conductance has the quantized plateaus  $2ne^2/h$  with  $n$  being an integer number. Unlike graphene and silicene nanoribbons, the conductances for both ZPNRs and APNRs are not symmetric with respect to the zero energy.



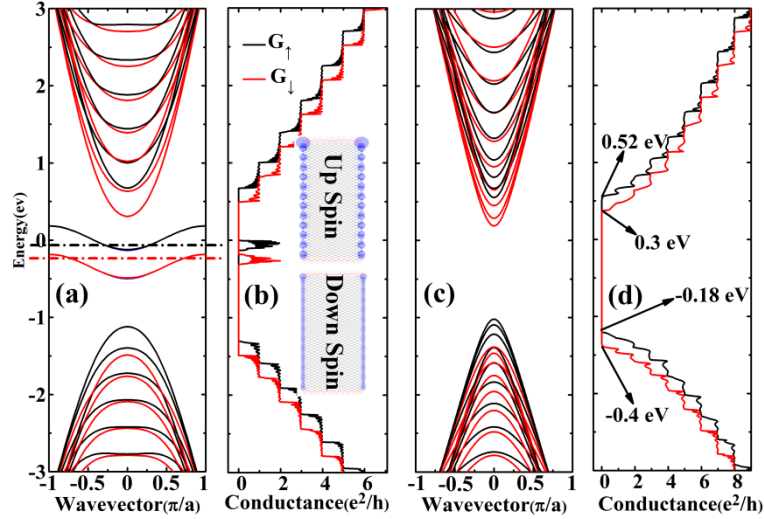


**Fig. 3** The spin-dependent band structure and their electron conductance in the normal/ferromagnetic/normal PNRs junctions. (a) and (b) The band structure and conductance for the ZPNRs. (c) and (d) The band structure and conductance for the APNRs. The inset in (b) is the LDOS for ZPNRs at  $E_F = -0.06$  eV (black dot-dash line in (a)) and  $E_F = -0.24$  eV (red dot-dash line in (a)) respectively. The exchange splitting is  $M=0.184$ eV, and the gate voltage is  $V_g = 0$ .

When a ferromagnetic layer is deposited on PNRs (see Fig. 1(a)), electrons in the device are polarized by the proximity induced exchange splitting. The spin-dependent band structure and conductance of ZPNRs (see Figs. 3(a) and (b)) and APNRs (see Figs. 3(c) and (d)) are shown in Fig. 3. In Fig. 3(a), it is noted that the in-gap bands are doubled, which corresponds to the spin up and spin down electrons respectively. We can see in Fig. 3(b) that the spin up conductance and spin down conductance are not the same due to the exchange splitting. In the Fermi energy region  $-0.14$  eV  $< E_F < 0$ , we only have spin up conductance, and the spin down electrons are all filtered. In the Fermi energy region  $-0.32$  eV  $< E_F < -0.18$  eV, all the spin up electrons are filtered, and we only have spin down conductance. The LDOS shown in Fig. 3 are determined at the two Fermi energies ( $E_F = -0.06$  eV and  $-0.24$  eV, shown by the black and red

dot-dash lines in Fig. 3) which lies in the up-spin and down-spin bands in the middle of the gap. The LDOS of these two states concentrates along the edges of the ribbon indicating that the current flows at these two energies are carried by the edge states localized along the edges. The band structure of APNRs with a ferromagnetic stripe is shown in Fig. 3(c). When a ferromagnetic stripe is deposited on APNRs, the bands are splitted into spin up bands and spin down bands. In Fig. 3(d), we note that the conductance for spin up and down electrons are not identical, which leads to a spin polarization in APNRs. What's more, large spin polarization can be obtained in the energy regions 0.3 eV~0.52 eV and -0.4 eV~-0.18 eV.

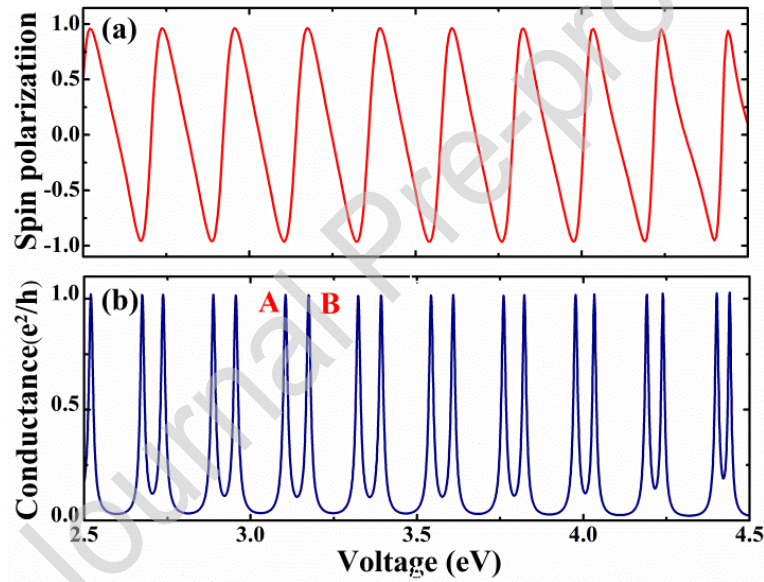


**Fig. 4.** (a) The spin polarization along  $z$  axis plotted as a function of an external gate voltage in the APNRs. (b) The total conductance plotted as a function of an external gate voltage in the APNRs. The other parameters are:  $E_F = 0.4$  eV,  $M = 0.184$  eV.

Next, we focus on the spin polarized transport in APNRs with a gate voltage applied, and the spin polarization and conductance are plotted as a function of gate voltage in Fig. 4. It is found that the spin polarization can be adjusted by the external

gate voltage, and the spin polarization oscillates periodically from -100% to 100% by a small change of the gate voltage. We can see in Fig. 4(a) that the spin polarization is rapidly reversed from positive to negative by changing the gate potential slightly. It provides us a method to control the direction of spin current in PNRs. The corresponding total conductance of the normal/ferromagnetic/normal PNRs junctions is presented in Fig. 4(b), and the conductance is plotted as a function of the gate voltage. It is found that the conductance has a series of resonance peaks. We can see that the two nearest peaks in the conductance corresponds to the negative and positive peaks in the spin polarization. For example, we have two nearest peaks A and B in Fig. 4(b), and we have the negative spin polarization peak at point A, and the positive spin polarization peak is found at point B. The spin polarization is reversed between the two points A and B.

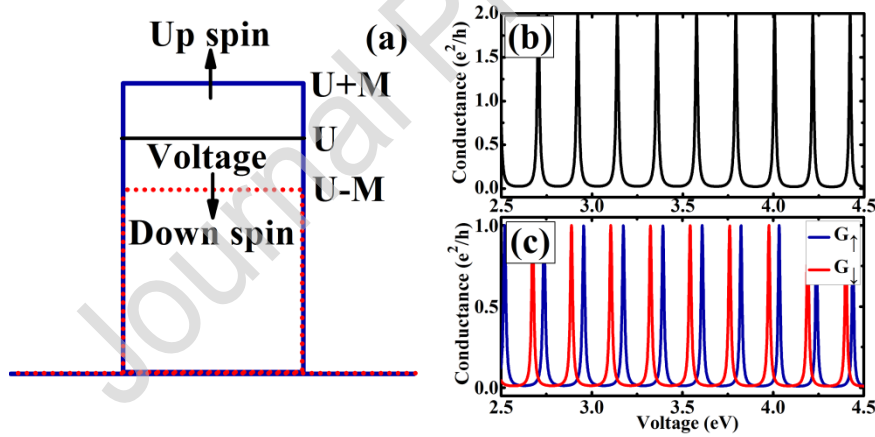


**Fig.5** (a) Potential barriers for the ferromagnetic PNRs with gate voltage. The potential barriers for spin up electrons (blue line) and spin down electrons (red line) are illustrated. (b) The conductance for our proposed device with only a gate potential barrier. (c) The spin resolved conductances are plotted as a function of the gate voltage. The parameters are the same as that in Fig. 4.

To understand the resonance peaks and switching of the spin polarization shown in Fig.4, we consider the potential barriers and the corresponding conductance for spin up and spin down electrons in Fig. 5. In our proposed device, both the gate voltage and the ferromagnetic stripe are considered, and the ferromagnetic stripe induces exchange splitting through proximity effect. There is no coupling between the spin up and spin down electrons, so it is easy for us to consider the potential barriers for spin up and spin down electrons separately. In Fig. 5(a), we can see that the spin up and spin down electrons see square barriers  $U+M$  and  $U-M$  respectively. When no ferromagnetic layer is considered, the conductance versus the gate voltage (the barrier height) has a series of resonance peaks as shown Fig. 5(b). For the spin up electrons, we also have a series of resonance peaks (see Fig. 5(c)), but the series of peaks are shifted from the series for the situation without ferromagnetic layer (see Fig. 5(b)). It is not surprising that the series of peaks for the spin down electrons shifted from the spin up series due to the different barrier height induced by the exchange splitting. Since the series of peaks for spin up electrons and spin down electrons appear at different gate voltages, the sign of spin polarization changes with respect to the gate voltages, which means that the spin direction can be changed by modulating the gate voltages.

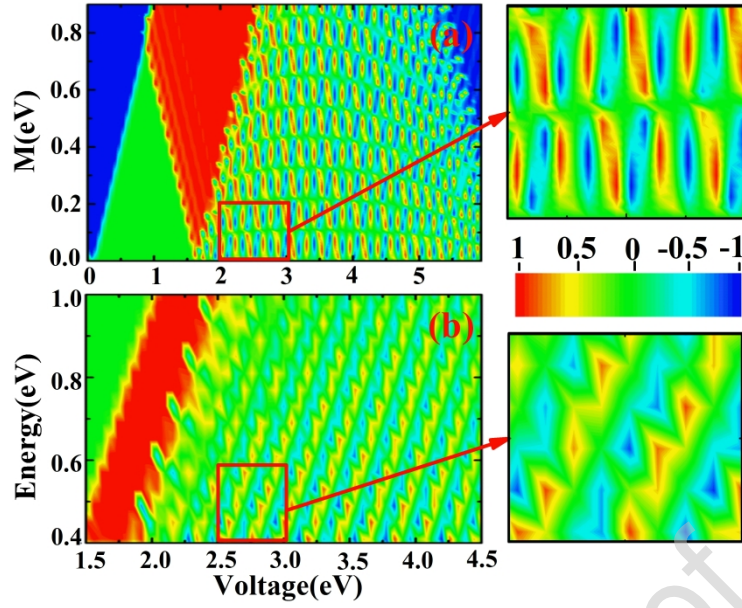


**Fig. 6.** (a) Contour plot of the spin polarization (red represents spin polarization=1, blue represents spin polarization =-1) as a function of the exchange field and gate voltage. The Fermi energy  $E_F = 0.4$  eV. (b) Contour plot of the spin polarization as a function of the Fermi energy and gate voltage. The exchange splitting is  $M = 0.184$  eV.

Lastly, we want to consider the numerical results for our proposed device with weaker or stronger ferromagnets, which is very important for the experimental realization. In Fig. 6(a), the spin polarization for APNRs is plotted as a function of the exchange field and gate voltage (blue (red) represents spin polarization=-1(1)). The exchange splitting varies from 0 to 0.9 eV which means that the effects of very weak and very strong ferromagnets are all included in the results. When the exchange splitting is small (around the bottom of Fig. 6(a)), the spin polarization also oscillates periodically from positive to negative, as the color of the plot oscillates between red (polarization=-1) and blue (polarization=1). This reversal of the spin polarization can be found in the top of Fig. 6(a) too, which means the switching of the spin polarization occurs for both small and large exchange fields. Although we use mainly

the value of 0.184 eV for the exchange splitting in other results, our prediction applies to both weak and strong ferromagnets according to Fig. 6(a). In Fig. 6(b), the spin polarization is plotted as a function of the Fermi energy and the gate voltage for a fixed exchange splitting of 0.184 eV. Boundary conditions for phosphorene nanoribbons in the continuum approach. We can see that the spin polarization oscillates with respect to the gate voltage in a wide range of Fermi energy. It is also noted that the amplitude of the spin polarization in the low energy region is larger than that in the higher energy region. For example, the amplitude of the spin polarization at  $E_F = 0.4$  eV can be as large as 100%, but the amplitude of the spin polarization is around 50% at  $E_F = 1$  eV.

## Conclusions

In summary, we have studied the spin polarized transport in PNRs under the influence of a proximity induced exchange splitting. The spin resolved conductance and spin polarization for the normal/ferromagnetic/normal PNR junctions are calculated and it is found that fully spin polarized current can be obtained in both armchair and zigzag PNRs. The gate-voltage-controllable spin polarization is obtained in the APNRs, and the spin polarization is found to be a sensitive oscillatory function of the gate voltage. The spin polarization can be easily reversed from 100% to -100% by a very small change in the external gate voltage. The switching of spin direction by a gate potential enables new possibilities for spin control in APNRs, which may stimulate further experimental investigations.

## Acknowledgements

This work was supported by the National Natural Science Foundation of China.(NSFC, Grant No. 11704078),Guangdong University of Technology One-HundredYoung Talents Program (Project No. 220413143).

## References

- [1] K.S. Novoselov, A.K. Geim, S.V. Morozov, D. Jiang, Y. Zhang, S.V. Dubonos, I.V. Grigorieva, A.A. Firsov, Electric Field Effect in Atomically Thin Carbon Films, *Science* 306 (2004) 666-669.
- [2] Y. Wu, Y.-m. Lin, A.A. Bol, K.A. Jenkins, F. Xia, D.B. Farmer, Y. Zhu, P. Avouris, High-frequency, scaled graphene transistors on diamond-like carbon, *Nature* 472 (2011) 74-78.
- [3] B. Radisavljevic, A. Radenovic, J. Brivio, V. Giacometti, A. Kis, Single-layer MoS<sub>2</sub> transistors, *Nat. Nanotechnol.* 6 (2011) 147-150.
- [4] Y. Yoon, K. Ganapathi, S. Salahuddin, How Good Can Monolayer MoS<sub>2</sub> Transistors Be?, *Nano Lett.* 11 (2011) 3768-3773.
- [5] K.F. Mak, C. Lee, J. Hone, J. Shan, T.F. Heinz, Atomically Thin MoS<sub>2</sub>: A New Direct-Gap Semiconductor, *Phys. Rev. Lett.* 105 (2010) 136805.
- [6] B. Lalmi, H. Oughaddou, H. Enriquez, A. Kara, S. Vizzini, B. Ealet, B. Aufray, Epitaxial growth of a silicene sheet, *Appl. Phys. Lett.* 97 (2010) 223109.
- [7] P. Vogt, P. De Padova, C. Quaresima, J. Avila, E. Frantzeskakis, M.C. Asensio, A. Resta, B. Ealet, G. Le Lay, Silicene: Compelling Experimental Evidence for Graphenelike Two-Dimensional Silicon, *Phys. Rev. Lett.* 108 (2012) 155501.
- [8] L. Chen, C.-C. Liu, B. Feng, X. He, P. Cheng, Z. Ding, S. Meng, Y. Yao, K. Wu, Evidence for Dirac Fermions in a Honeycomb Lattice Based on Silicon, *Phys. Rev. Lett.* 109 (2012) 056804.
- [9] C.J. Tabert, E.J. Nicol, Magneto-optical conductivity of silicene and other buckled honeycomb lattices, *Phys.Rev. B* 88 (2013) 085434.

- [10] M.S. Fuhrer, J. Hone, Measurement of mobility in dual-gated MoS<sub>2</sub> transistors, Nat. Nanotechnol. 8 (2013) 146-147.
- [11] D. Xiao, G.-B. Liu, W. Feng, X. Xu, W. Yao, Coupled Spin and Valley Physics in Monolayers of MoS<sub>2</sub> and Other Group-VI Dichalcogenides, Phys. Rev. Lett. 108 (2012) 196802.
- [12] L.K. Li, Y.J. Yu, G.J. Ye, Q.Q. Ge, X.D. Ou, H. Wu, D.L. Feng, X.H. Chen, Y.B. Zhang, Black phosphorus field-effect transistors, Nat. Nanotechnol. 9 (2014) 372-377.
- [13] H. Liu, A.T. Neal, Z. Zhu, Z. Luo, X. Xu, D. Tomanek, P.D. Ye, Phosphorene: An Unexplored 2D Semiconductor with a High Hole Mobility, Acs Nano 8 (2014) 4033-4041.
- [14] A. Castellanos-Gomez, L. Vicarelli, E. Prada, J.O. Island, K.L. Narasimha-Acharya, S.I. Blanter, D.J. Groenendijk, M. Buscema, G.A. Steele, J.V. Alvarez, H.W. Zandbergen, J.J. Palacios, H.S.J. van der Zant, Isolation and characterization of few-layer black phosphorus, 2D Mater. 1 (2014) 025001.
- [15] E.S. Reich, Phosphorene excites materials scientists, Nature 506 (2014) 19.
- [16] A.S. Rodin, A. Carvalho, A.H. Castro Neto, Strain-Induced Gap Modification in Black Phosphorus, Phys. Rev. Lett. 112 (2014) 176801.
- [17] K.S. Novoselov, A.K. Geim, S.V. Morozov, D. Jiang, M.I. Katsnelson, I.V. Grigorieva, S.V. Dubonos, A.A. Firsov, Two-dimensional gas of massless Dirac fermions in graphene, Nature 438 (2005) 197-200.
- [18] S. Das, W. Zhang, M. Demarteau, A. Hoffmann, M. Dubey, A. Roelofs, Tunable Transport Gap in Phosphorene, Nano Lett. 14 (2014) 5733-5739.
- [19] F. Xia, H. Wang, Y. Jia, Rediscovering black phosphorus as an anisotropic layered material for optoelectronics and electronics, Nat. Commun. 5 (2014) 4458.
- [20] X. Peng, A. Copple, Q. Wei, Edge effects on the electronic properties of phosphorene nanoribbons, J Appl. Phys. 116 (2014) 144301.
- [21] T. Vy, R. Soklaski, Y. Liang, L. Yang, Layer-controlled band gap and anisotropic excitons in few-layer black phosphorus, Phys.Rev. B 89 (2014) 235319.
- [22] M. Ezawa, Topological origin of quasi-flat edge band in phosphorene, New J. Phys. 16 (2014) 115004.



- [23] E.T. Sisakht, M.H. Zare, F. Fazileh, Scaling laws of band gaps of phosphorene nanoribbons: A tight-binding calculation, *Phys.Rev. B* 91 (2015) 085409.
- [24] B. Ostahie, A. Aldea, Phosphorene confined systems in magnetic field, quantum transport, and superradiance in the quasiflat band, *Phys.Rev. B* 93 (2016) 075408.
- [25] Q. Wu, L. Shen, M. Yang, Y. Cai, Z. Huang, Y.P. Feng, Electronic and transport properties of phosphorene nanoribbons, *Phys.Rev. B* 92 (2015) 035436.
- [26] J. Zhang, H.J. Liu, L. Cheng, J. Wei, J.H. Liang, D.D. Fan, J. Shi, X.F. Tang, Q.J. Zhang, Phosphorene nanoribbon as a promising candidate for thermoelectric applications, *Sci. Rep.* 4 (2014) 6452.
- [27] H. Guo, N. Lu, J. Dai, X. Wu, X.C. Zeng, Phosphorene Nanoribbons, Phosphorus Nanotubes, and van der Waals Multilayers, *J. Phys. Chem. C* 118 (2014) 14051-14059.
- [28] M. Kurpas, M. Gmitra, J. Fabian, Spin properties of black phosphorus and phosphorene, and their prospects for spin calorics, *J. Phys. DAppl. Phys.* 51 (2018) 174001.
- [29] Z.Y. Wang, C. Tang, R. Sachs, Y. Barlas, J. Shi, Proximity-Induced Ferromagnetism in Graphene Revealed by the Anomalous Hall Effect, *Phys. Rev. Lett.* 114 (2015) 016603.
- [30] P. Wei, S. Lee, F. Lemaitre, L. Pinel, D. Cutaia, W. Cha, F. Katmis, Y. Zhu, D. Heiman, J. Hone, J.S. Moodera, C.-T. Chen, Strong interfacial exchange field in the graphene/EuS heterostructure, *Nat. Mater.* 15 (2016) 711.
- [31] H. Chen, B. Li, J. Yang, Proximity Effect Induced Spin Injection in Phosphorene on Magnetic Insulator, *ACS Appl. Mater. Interfaces* 9 (2017) 38999-39010.
- [32] M.A.M. Keshtan, M. Esmailzadeh, Spin filtering in a magnetized zigzag phosphorene nanoribbon, *J. Phys. D-Appl. Phys.* 48 (2015) 485301.
- [33] H.H. Fu, D.D. Wu, L. Gu, M.H. Wu, R.Q. Wu, Design for a spin-Seebeck diode based on two-dimensional materials, *Phys.Rev. B* 92 (2015) 045418.
- [34] A.N. Rudenko, M.I. Katsnelson, Quasiparticle band structure and tight-binding model for single- and bilayer black phosphorus, *Phys.Rev. B* 89 (2014) 201408.
- [35] E.T. Sisakht, F. Fazileh, M.H. Zare, M. Zarenia, F.M. Peeters, Strain-induced

topological phase transition in phosphorene and in phosphorene nanoribbons, Phys. Rev. B. 94 (2016) 085417.

[36] R. Ma, H. Geng, W.Y. Deng, M.N. Chen, L. Sheng, D.Y. Xing, Effect of the edge states on the conductance and thermopower in zigzag phosphorene nanoribbons, Phys. Rev. B, 94 (2016) 125410.

[37] D.J.P. de Sousa, L.V. de Castro, D.R. da Costa, J.M. Pereira, Boundary conditions for phosphorene nanoribbons in the continuum approach, Phys. Rev. B, 94 (2016) 235415.

[38] L.L. Li, F.M. Peeters, Quantum transport in defective phosphorene nanoribbons: Effects of atomic vacancies, Phys. Rev. B, 97 (2018) 075414.

[39] C.W. Groth, M. Wimmer, A.R. Akhmerov, X. Waintal, Kwant: a software package for quantum transport, New J. Phys. 16 (2014) 063065.

## Declaration of interest

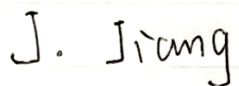
We wish to confirm that there are no known conflicts of interest associated with this publication and there has been no significant financial support for this work that could have influenced its outcome.

We confirm that the manuscript has been read and approved by all named authors and that there are no other persons who satisfied the criteria for authorship but are not listed. We further confirm that the order of authors listed in the manuscript has been approved by all of us.

We confirm that we have given due consideration to the protection of intellectual property associated with this work and that there are no impediments to publication, including the timing of publication, with respect to intellectual property. In so doing we confirm that we have followed the regulations of our institutions concerning intellectual property.

We understand that the Corresponding Author is the sole contact for the Editorial process (including Editorial Manager and direct communications with the office). He/she is responsible for communicating with the other authors about progress, submissions of revisions and final approval of proofs. We confirm that we have provided a current, correct email address which is accessible by the Corresponding Author and which has been configured to accept email from [qtzhang@mail.ustc.edu.cn](mailto:qtzhang@mail.ustc.edu.cn).

Signed by all authors as follows:



Junsong Jiang 8-10-2019



Qingtian Zhang 8-10-2019



Zhongfei Mu 8-10-2019



K S Chan 8-10-2019

**Highlights**

We investigate the spin polarized transport in phosphorene nanoribbon with a ferromagnetic stripe.

Fully spin polarized current can be obtained in both zigzag and armchair phosphorene nanoribbons.

The spin polarization for armchair phosphorene nanoribbon oscillates periodically from positive to negative by a slight change of the gate voltage.

The switching of spin direction by a gate potential has useful applications in the development of spintronic devices.